Vol. 682: 65–77, 2022
https://doi.org/10.3354/meps13921

MARINE ECOLOGY PROGRESS SERIES
Mar Ecol Prog Ser

Published January 20

Grazing of a heterotrophic nanoflagellate on prokaryote and eukaryote prey: ingestion rates and gross growth efficiency

Gabrielle L. Corradino[1,2,*], Astrid Schnetzer[1]

[1]Department of Marine, Earth and Atmospheric Sciences, North Carolina State University, Raleigh, NC 27695, USA

[2]*Present address:* Office of Education Headquarters, National Oceanic and Atmospheric Administration, Washington, DC 20230, USA

ABSTRACT: Heterotrophic nanoflagellates (HNANs) play a pivotal role as consumers of picoplankton, remineralizers and carbon vectors, yet knowledge on how prey quantity and quality affect HNAN physiology remains limited. In a series of grazing experiments using an uncharacterized member of the HNAN assemblage, we found that growth (μ) and ingestion rate (IR) varied when offering heterotrophic bacteria (HB), *Synechococcus* spp. (*Syn*), *Ostreococcus lucimarinus* (*Ost*) or a combination of all 3 prey types. Highest average μ rates (1.8 d^{-1}) were detected on HB at densities of ~10^6 cells ml^{-1} and maximum IR on *Syn* (485 pg C d^{-1}) at ~10^6 cells ml^{-1}. Independent of prey type, flagellate μ increased with IR up to ~50 pg C d^{-1}. A relatively low P-content in *Ost* was linked to shifts in C:N:P ratios of the HNAN in the single-prey experiment and when *Ost* was offered as part of the mixed assemblage. Presented with a mixed diet, the highest contribution to daily C intake came from *Ost* with 50%, followed by HB with 46% and *Syn* with only 4%. C-based gross growth efficiencies (GGEs) were higher when feeding on HB and mixed prey, compared to both picophototrophs, while N- and P-based GGEs in mixed prey treatments markedly exceeded those when feeding on any single prey. The findings in this study corroborate the importance of investigating the biogeochemical role of HNANs in relation to prey availability and quality to refine estimates of energy transfer within the microbial loop.

KEY WORDS: Heterotrophic nanoflagellate · Ingestion rate · Grazing · Gross growth efficiency

1. INTRODUCTION

Heterotrophic nanoflagellates (HNANs, 2–20 μm in size) are important grazers of picoplankton (0.2–2 μm) throughout the oceans and play pivotal roles in biogeochemical cycling within microbial food webs (Pomeroy 1974, Azam et al. 1983, Pernthaler 2005). Flagellate grazing may account for the daily removal of as little as ~5% but up to 100% of bacterial standing stocks, typically constituting the primary cause of bacterial mortality (vis-à-vis viral lysis) (Caron et al. 1999, Christaki et al. 2001, Tsai et al. 2013). Similarly, the extent to which heterotrophic flagellates exert top-down control over picophytoplankton (e.g. *Synechococcus* spp.) may range markedly, with 1–93% of biomass consumed daily (Safi & Hall 1999, Worden et al. 2004, Karayanni et al. 2005, Worden 2006). Both laboratory and field studies have demonstrated how prey quantity and quality may affect rates of flagellate community grazing (Gonzalez et al. 1990, Dolan & Šimek 1999, Christaki et al. 2001). Some studies also found that feeding ecologies and preferences differ among individual nanoflagellate species (Boenigk & Arndt 2000, Schnepf & Kühn 2000, Christaki et al. 2005). For instance, ingestion rates (IRs) for *Cafeteria* and *Ochromonas* were found to differ

*Corresponding author: gcorrad@ncsu.edu

depending on prey type, and IRs for *Ochromonas* exceeded those for *Cafeteria* by orders of magnitude when feeding on the same prey (Boenigk et al. 2001).

Variability in flagellate bacterivory has been attributed to prey size and mobility, with larger, mobile cells being ingested at higher rates (Gonzalez et al. 1990, Boenigk et al. 2001). Next to prey size as a potential indicator of nutritional value, some studies have also examined nutrient composition (C, N and P budgets) to aid in interpreting flagellate–prey dynamics (Eccleston-Parry & Leadbeater 1995, Grover & Chrzanowski 2009). Previous work has shown that the typical C:N:P ratio for HNANs may range from 6:1.5:1 to 66:10:1 and can shift based on the nutrient composition of ingested prey (Eccleston-Parry & Leadbeater 1995, Chrzanowski & Foster 2014). A growing number of studies emphasize the role that phototrophic prey, mainly cyanobacteria *Synechococcus* (*Syn*) and *Prochlorococcus* spp., play in flagellate diet next to feeding on heterotrophic bacteria (HB) (Dolan & Šimek 1998, 1999, Guillou et al. 2001, Christaki et al. 2002), and a few have examined nanoflagellate feeding on picoeukaryotes, mainly *Ostreococcus* (*Ost*) and *Choricystis* spp. (Christaki et al. 2005, Bręk-Laitinen & Ojala 2011). Generally, HNANs are able to ingest varying phototrophs; however, their ability to sustain population growth (μ) on such diets seems to differ between flagellate species (Dolan & Šimek 1998, Christaki et al. 2001, Bec et al. 2006).

Prey quantity and quality can impact flagellate μ and may also affect gross growth efficiency (GGE), the amount of prey carbon (C) converted into HNAN biomass (Straile 1997, Dahlgren et al. 2010). While C-based GGEs for HNANs feeding on natural prey communities typically fall between 23 and 54% (Fenchel 1982a, Børsheim & Bratbak 1987, Rose et al. 2009), laboratory studies have reported variations dependent on prey and grazer 'matches'. For instance, in experiments where the same prey (*E. coli*) was offered to differing flagellates, maximum GGE for *Pteridomonas* sp. reached 22%, while values were twice as high (~43%) for *Ochromonas* sp. (Wikner et al. 1986, Pelegrí et al. 1999). In another example, grazing on various strains of *Syn*, the HNAN *Goniomonas pacifica* yielded GGEs from 13 to 45% (Apple et al. 2011). A limited number of investigations have extended nutrient measurements to include N and P to calculate GGEs (Caron et al. 1990, Eccleston-Parry & Leadbeater 1995, Chrzanowski et al. 2010). Christaki et al. (2005) also reported decreases in biovolume (BV) of certain flagellates feeding on prey like the picoeukaryote *Ostreococcus* compared to HB. A growing number of studies continues to provide better insight into how the biogeochemical roles of HNANs link to grazer-specific and prey-dependent responses.

The objective of this study was to examine grazing and μ of a recently isolated nanoflagellate, herein referenced as HNAN. The flagellate, a likely member of the order Bicosoecida (full characterization pending), had originally been isolated from the North Carolina (USA) coast. Grazing was examined for 3 common prey types/groups including a mixed HB assemblage, the cyanobacterium *Syn* and the picoeukaryote *Ost*. Prey was offered over increasing concentrations (~10^3 to 10^6 cells ml^{-1}) in separate short-term incubations (24 h), and then all prey types were combined to examine HNAN feeding on the mixed assemblage. The effects of prey concentration and type on the HNAN μ, IRs, predator BV and GGE are discussed.

2. MATERIALS AND METHODS

2.1. Predator origins and culture conditions

Plankton surface tows (150 μm mesh size) were conducted in the eastern part of Bogue Sound, North Carolina, USA, during October 2015 (34° 43′ 17.77″ N, 76° 45′ 33.93″ W). The tows were originally targeting varying microphytoplankton, and the nanoflagellate was isolated attached to diatom cells. The diatoms were grown in F/20 medium (Guillard & Ryther 1962) at 22°C and a light:dark (L:D) cycle of 14:10 h at 75 μE m^{-2} s^{-1} using cool white fluorescent light. The flagellates tended to numerically dominate the diatom cultures within 2 wk of each transfer. The ~5 μm-sized cells were separated from the microalgae using a 20 μm Nitex mesh screen combined with a series of dilution steps. Once isolated, the nanoflagellate assemblage was grown at 14:10 h L:D cycle with F/20 and in the dark with a barley seed. While these initial cultures contained a mix of pigmented and colorless flagellates, dark growth conditions exclusively selected non-pigmented cells, and further examination via epifluorescence microscopy confirmed that after several months in the dark, transferring the flagellate back to original growth conditions (14:10 h L:D cycle plus F/20 and/or barley seed) did not result in the return of pigmented cells.

To determine whether a single or several heterotrophic species were present, aliquots of 100 ml from the cultures were concentrated onto 25 mm GF/F filters (0.7 μm pore size) and stored at –20°C. The DNA

was extracted using a DNA Isolation Kit (MoBio, Qiagen), and the 18S rDNA was partially amplified using universal eukaryotic primers 575 FWD (5′-GTA ATT CCA GCT CCA ATA GC-3′) (Weekers et al. 1994) and NS4 (5′-CTT CCG TCA ATT CCT TTA AG-3′) (White et al. 1990). Briefly, the PCR reaction contained 5 µl of template DNA, 1 µl 0.1 µM of each primer, 18 µl of nuclease-free water and 2× DreamTaq Green PCR Master Mix (DreamTaq DNA polymerase, 2× Green buffer, 0.4 mM of each dNTP, 4 mM $MgCl_2$) (ThermoScientific) for a total volume of 50 µl. The PCR was run (Thermocycler, BioRad) using an initial denaturation step for 10 min at 95°C, followed by 35 cycles of 30 s at 94°C, 30 s at 55°C, and 1 min at 72°C, with an extension for 8 min at 72°C. The PCR products were cleaned and then ligated using a cloning kit (Qiagen) following the manufacturer's instructions using electro-competent cells (Thermofisher, OneShot Top 10) and electroporation (Gene Pulser Xcell, BioRad) and sent out for sequencing (n = 10). All sequencing was conducted using outside services (SimpleSeq, Eurofin).

2.2. Prey origins

Cultures of *Syn* (NCMA 2370), *Ost* (NCMA 3430) and a freshly isolated mixed assemblage of HB were used as prey. The HB assemblage was collected from the same location as the flagellate. The bacteria were grown in the dark at 16°C (*in situ* temperature during isolation) with 0.2 µm-aged seawater with F/2 and a single barley seed (Guillard & Ryther 1962), transferred every 6 d and used in the feeding experiments within 60 d of collection. *Syn* and *Ost* were grown under a 14:10 L:D cycle (75 µE m^{-2} s^{-1}) with F/2 (Guillard & Ryther 1962) as was the nanoflagellate with the addition of a baked barley seed.

2.3. Grazing experiment

Feeding experiments (24 h) were conducted at 16°C to examine HNAN µ (d^{-1}), IRs (cells flagellate (flag)$^{-1}$ d^{-1} and fg C^{-1} $flag^{-1}$ d^{-1}), shifts in HNAN BV (µm^3 $cell^{-1}$) and cell stoichiometry (C, N and P). The incubation temperature was chosen based on the original isolation temperature for the HNAN. Exponentially growing HB, *Syn* and *Ost* were each inoculated with the flagellate and, on one occasion, combined to provide a mixed prey assemblage. Prey–predator and control treatments were set up in triplicates where each flask contained a total volume of 170 ml of artificial seawater (ASW; ASTM D1141-98, Lake Products), spiked initially with F/2 to account for prey growth due to the availability of remineralized nutrients in bottles with the HNAN compared to the control treatments (Selph et al. 2003). Initial prey concentrations for each of the 3 prey types ranged from ~10^3 to 10^6 cells ml^{-1} (Table 1). The control treatments were run at ~10^5 cells ml^{-1} for each of the prey items (no flagellate added). For the mixed prey experiment, starting concentrations were ~10^5 cells ml^{-1} for the mixed HB assemblage and ~10^3 cells ml^{-1} for both *Syn* and *Ost* cultures (Table 1), based on concentrations typical for coastal waters (Olson et al. 1990, Countway & Caron 2006). The flagellate was gently concentrated using a 3 µm filter by passive filtration and then transferred into 0.2 µm-filtered ASW ~2 h prior to all experiments to allow for emptying of food vacuoles under decreased concentrations of background bacteria at ~10^2 to 10^3 ml^{-1} (Šimek & Chrzanowski 1992, Bratvold et al. 2000, Zwirglmaier et al. 2009). Samples to determine cell abundances for the HNAN and the prey were obtained at the beginning (T0), after 12 h (T1) and after 24 h (TF). Using a nanoplankton chamber (PhycoTech), triplicate subsamples (10 µl) from each flask were used to enumerate HNAN abundances live using light microscopy

Table 1. Mean ± SD initial prey and predator abundances (cells ml^{-1}) in each of the 4 experiments. Prey densities in the control flasks started at ~10^6 cells ml^{-1} (no flagellate added). HNAN: heterotrophic nanoflagellate; HB: heterotrophic bacteria; *Syn*: *Synechococcus*; *Ost*: *Ostreococcus lucimarinus*; Mix: mixed prey assemblage

Treatment	HNAN (×10^2)	Prey	Prey in control
HB	4.6 ± 0.5	3.4 ± 0.01 (×10^3)	1.3 ± 0.2 (×10^5)
	4.7 ± 0.6	1.8 ± 0.04 (×10^4)	
	2.8 ± 0.3	1.7 ± 0.2 (×10^5)	
	5.3 ± 0.6	0.9 ± 0.3 (×10^6)	
Syn	2.8 ± 2.8	1.1 ± 0.1 (×10^3)	0.1 ± 0.03 (×10^5)
	2.0 ± 0.0	2.2 ± 1.2 (×10^4)	
	2.8 ± 2.8	1.5 ± 0.2 (×10^5)	
	3.0 ± 0.0	10.0 ± 0.1 (×10^6)	
Ost	6.4 ± 3.1	2.2 ± 0.1 (×10^3)	4.1 ± 0.5 (×10^5)
	4.3 ± 1.1	3.7 ± 0.6 (×10^4)	
	5.3 ± 3.0	5.3 ± 1.2 (×10^5)	
	5.7 ± 2.0	0.7 ± 0.5 (×10^6)	
Mix	17.6 ± 3.0	HB 0.7 ± 0.5 (×10^5)	0.8 ± 0.2 (×10^5)
		Syn 2.1 ± 0.6 (×10^3)	3.3 ± 0.1 (×10^3)
		Ost 2.5 ± 1.0 (×10^3)	2.7 ± 0.2 (×10^3)

(BX53, Olympus, Japan) under differential interference contrast. Picoplankton were enumerated using 3 ml from each triplicate flask after preservation with ice-cold 2% glutaraldehyde and, in the case of the HB, staining with DAPI (Slowfade gold antifade, Thermofisher) (Porter & Feig 1980). The picoplankton prey were quantified under 60 and 100× magnification using epifluorescence microscopy. Samples to determine HNAN BV (30 µl) and elemental composition (150 ml combined from each of the triplicate bottles) were collected at T0 and at TF for the control bottles (prey only), and in grazer treatments were measured within the first hour of feeding and then after 24 h at TF.

2.4. Flagellate growth, ingestion rates and biovolumes

Calculations of µ rates and IRs were based on the equations of Frost (1972) modified by Heinbokel (1978), to account for the growth of the HNAN between sampling.

Cell size estimates for the nanoflagellate and prey were obtained by measuring cells preserved in glutaraldehyde and capturing images (n = 30 for HNAN and n = 40 for the prey in each treatment and at each time point) with an Olympus DP73 monochrome digital camera plus Olympus cellSens Dimension 1.13 software. Comparison with live flagellate cells indicated 24–30% cell shrinkage with preservation, which is within the range of previously reported values for flagellates (Hondeveld et al. 1992). HNAN BV was calculated using the ellipsoid equation of (Hillebrand et al. 1999). BVs for HB were estimated by applying cone or ellipsoid shapes. Shapes for *Syn* and *Ost* were approximated as ellipsoids.

2.5. Elemental ratios and GGE

Nutrient samples were collected at T0 and TF from flasks that contained HB, *Syn*, *Ost* and the mixed prey assemblage. To accumulate sufficient biomass, subsamples from 3 treatment bottles were combined (total of 150 ml) and filtered onto precombusted 0.2 µm filters. For the single-prey experiments, these samples were collected from treatment bottles containing ~10^5 cells ml^{-1}. Each of the GF/F filters was individually stored in a petri dish at −20°C for ~5 wk prior to elemental analysis. Briefly, particulate carbon and particulate nitrogen concentrations were determined following modified methods of Froelich (1980). Each filter was wrapped in methanol-cleaned tin boats and combusted at 1000°C in a Perkin Elmer 2400 elemental analyzer. Total particulate phosphorus was determined using a modification of the method reported by Aspila et al. (1976). Filters were combusted at 550°C to convert all organic P present into inorganic P forms and extracted using a weak hydrochloric acid (Aspila et al. 1976, Benitez-Nelson et al. 2007). A standard reference material (NIST #1573a, tomato leaves) was analyzed with each run to evaluate analytical accuracy and monitor run to run variability. HNAN cell nutrient contents were calculated by correcting total estimates for C, N and P values for prey. For this, prey cell content values for each prey type (control bottles) were multiplied by prey cell abundance in the varying grazer bottles and subtracted. Finally, changes in C:N, N:P and C:P ratios were examined for each prey type and the flagellate.

GGEs of the HNAN were calculated following the equation of Choi & Peters (1992) based on abundance and C, N and P biomass change in the cultures in relation to changes for the HNAN abundances (Fenchel 1982b, Choi & Peters 1992).

2.6. Statistical analyses

Statistical analyses were performed using the JMP Pro 14 software package (SAS Institute). Differences in µ, IR and GGE among treatments were examined using a 1-way ANOVA (Zar 1984). Means were compared using a Tukey test (results were considered significant at $p < 0.05$).

3. RESULTS

3.1. Nanoflagellate characterization

Initial sequencing of the 575Fwd region consisting of read lengths from 450 to 1000 bp resulted in sequence similarities of 100% for 9 out of the 10 clones, with 1 clone showing a 1-base difference (99% similarity), indicating the presence of a single species (GenBank accession numbers MZ676996–MZ677004). BLAST results returned the closest matches (≤96% sequence similarities) to uncultured eukaryotes from marine environments from the Aegean Sea (AY789790.1), Caribbean Sea (GU-823081.1) and the Black Sea (HM749932.1). The closest match to a previously identified organism based on NCBI only returned an 89.6% match to *Bicosoeca*

vacillans (AY520445.1) and an 89% match to *Filos agilis* (FJ971856.1), generally placing the organism within the order of Bicosoecida. A full characterization of the organism, encompassing sequencing of the full length 18S gene and additional gene targets as well as ultrastructure analyses via electron microscopy, are currently underway.

3.2. Prey and predator BV and cell stoichiometry

No significant changes were detected for cell BV over time for any of the prey organisms in the control treatments ($p > 0.05$). At T0, *Syn* cell size averaged 0.9 ± 0.9 (SD) µm^3 (n = 40) and *Ost* 3.1 ± 1.1 µm^3 (n = 40), and at TF, *Syn* and *Ost* cell size was 1.3 ± 0.9 and 3.3 ± 1.0 µm^3 cell^{-1}, respectively (Fig. 1). For HB, a decrease in BV from 1.4 ± 1.7 to 0.4 ± 0.8 µm^3 cell^{-1} was indicated; however, this overall change was not statistically significant ($p > 0.05$) (Fig. 1). The initial BV for HNAN averaged 36 ± 10 µm^3 cell^{-1} and changed when the flagellate was fed *Syn* (Fig. 2). In this treatment, BVs increased to 64 ± 17 µm^3 cell^{-1} by TF (n = 30 for each time point; $p < 0.05$; Fig. 2). Grazer BVs also increased when feeding on the mixed assemblage, averaging 68 ± 26 µm^3 cell^{-1} (n = 30). These shifts in predator size were already observable after the first 12 h of each experiment (T1 in Fig. 2).

For the computation of C-based IR and GGEs, prey nutrient contents were computed per cell and per BV by averaging T0 and TF values (Table 2). Estimates for the HB were determined with 55 fg C µm^{-3}, 9 fg N µm^{-3} and 4 fg P µm^{-3} (Table 2). Estimates were 181 fg C µm^{-3}, 37 fg N µm^{-3} and 6 fg P µm^{-3} for *Syn*, and 656 fg C µm^{-3}, 37 fg N µm^{-3} and 6 fg P µm^{-3} for *Ost* (Table 2). HNAN nutrient contents were averaged

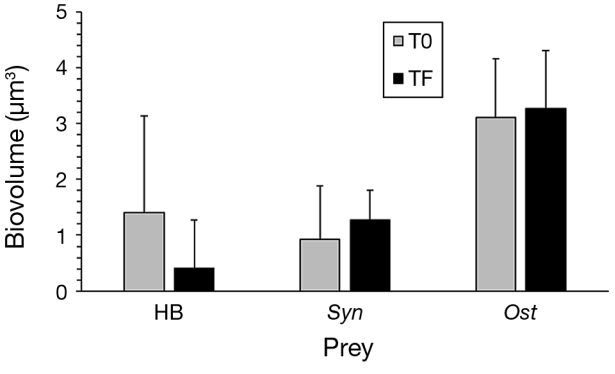

Fig. 1. Average cell biovolume (BV; µm^{-3} cell^{-1}; +SD) of the prey at the beginning (T0) and end (TF, 24 h) of the experiment (n = 40 each). HB: heterotrophic bacteria; *Syn*: *Synechococcus*; *Ost*: *Ostreococcus lucimarinus*

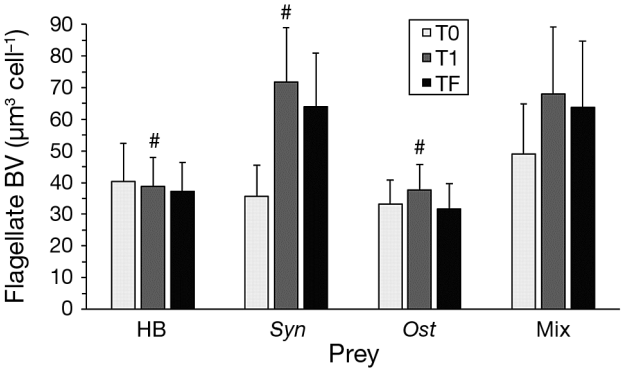

Fig. 2. Average cell biovolume (BV) of the flagellate fed on various prey (n = 30; +SD). # denotes a significant difference between the beginning (T0) and 12 h (T1) or 24 h (TF) cultures ($p < 0.05$). Mix: mixed prey assemblage; other abbreviations as in Fig. 1

Table 2. Averaged prey carbon (C), nitrogen (N) and phosphorus (P) content in fg cell^{-1} and normalized by biovolume in fg µm^{-3} in the control treatments. HB: heterotrophic bacteria; *Syn*: *Synechococcus*; *Ost*: *Ostreococcus lucimarinus*; Mix: mixed prey assemblage

Prey	C	N	P	C	N	P
	fg cell^{-1}			fg µm^{-3}		
HB	77	12	5	55	9	4
Syn	230	48	7	181	37	6
Ost[a]	2144	122	18	656	37	6
Mix	222	37	11	202	34	10

[a]For *Ost*, cell content estimates were available for initial (T0) observations only

using values collected approximately ~1 h into the experiments and at TF (Table 3). Feeding on *Ost*, HNAN C content averaged 495 fg C µm^{-3}, followed by the flagellate fed on HB with 403 fg C µm^{-3}, 330 fg C µm^{-3} for *Syn* and 214 fg C µm^{-3} for flagellates fed on the mixed assemblage (Table 3). Molar elemental ratios (C:N:P) for each prey organism were similar for HB and *Syn*, with 14:2:1 and 31:7:1, but deviated from *Ost* with 119:7:1, indicating a higher C content for *Ost* in relation to N and especially P (C:N = 17.6 and C:P = 119; Table 4). In the single-prey treatments, HNAN feeding on *Ost* yielded similar C:N values (overall range = 7–9) but N:P and C:P ratios were relatively high at 10 and 64 compared to the other treatments, reflecting differences in prey nutrient composition (i.e. low P content for *Ost*; Fig. 3, Table 4). Moreover, C:N:P results for HNAN feeding on the mixed prey treatments (including *Ost*) yielded ratios that fell in between single-prey estimates for HB and *Syn* compared to the *Ost* single-prey treatments (Table 4).

Table 3. Carbon (C), nitrogen (N) and phosphorus (P) cell content and molar elemental ratios for the flagellate. Cell contents for flagellate grazing on varying prey (mixed heterotrophic bacteria [HB], *Synechococcus* [*Syn*], *Ostreococcus* [*Ost*] and mixed [Mix] treatments) are shown in pg cell^{-1} and normalized by biovolume in fg µm^{-3}. Flagellate nutrient concentrations are shown in comparison to estimates reported elsewhere. Values are averages from at least 2 or more observations. HNAN: heterotrophic nanoflagellate; Bact Cult: bacterial culture; (–): data unavailable

Nanoflagellate(s)	Prey	C	N	P	C:N	C:N:P	C	N	P	Source
		— pg cell^{-1} —					— fg µm^{-3} —			
Unknown HNAN	HB	15	2	0.9	8.5	17:02:01	406	47	27	This study
	Syn	15	2	1.3	8.3	12:01:01	330	30	16	
	Ost	19	3	0.3	6.6	64:10:01	495	272	38	
	Mix	9	0.9	0.2	10.4	39:04:01	214	14	3	
Paraphysomonas imperforata	HB	32.5	7.4	1.2	4.5	27:06:01	149	35	6	Eccleston-Parry & Leadbeater (1995)
Bodo designis	HB	12.6	3.1	2.2	4.1	01:05.5	233	57	41	
Stephanoeca diplocostata	HB	5.4	1.1	0.1	4.9	45:09:01	156	31	3	
Jakoba libera	HB	14.2	2.6	0.2	5.5	71:13:01	189	34	3	
Ochromonas danica[a]	Bact Cult	32.8	2.6	0.6	18.2	161:10:01	386	31	7	Chrzanowski et al. (2010)
	Bact Cult	46.6	7.9	1.5	6.9	80:12:01	885	150	28	Chrzanowski et al. (2010)
	Bact Cult	–	–	–	–	66:10:01	–	–	–	Chrzanowski & Foster (2014)
Paraphysomonas spp.	Bact Cult	–	–	–	5	–	466	93	–	Sin et al. (1998)
	Bact Cult	–	–	–	10.6	–	181	17	–	
Paraphysomonas bandaiensis	HB	–	–	–	5.2	–	130	–	–	
Monas sp.[b]	Bact Cult	–	–	–	4.6	–	100	–	–	Børsheim & Bratbak (1987)
	Bact Cult	–	–	–	4.6	–	220	–	–	

[a]Study used bacteria raised under balanced growth conditions and under C limitation
[b]C content differences for the same organisms linked to cell shrinkage during preservation

Table 4. Elemental ratios for prey and the flagellate fed on each prey type (n = 2). HB: heterotrophic bacteria; *Syn*: *Synechococcus*; *Ost*: *Ostreococcus lucimarinus*; Mix = mixed prey assemblage; HNAN: heterotrophic nanoflagellate

	C:N:P	C:N	N:P	C:P
Prey (Control)				
HB	14:02:01	7	2	14
Syn	31:07:01	5	7	31
Ost	119:07:01	18	7	119
Mix	21:04:01	6	4	21
HNAN fed on				
HB	17:02:01	9	2	17
Syn	12:01:01	8	1	12
Ost	64:10:01	7	10	64
Mix	39:04:01	10	4	39

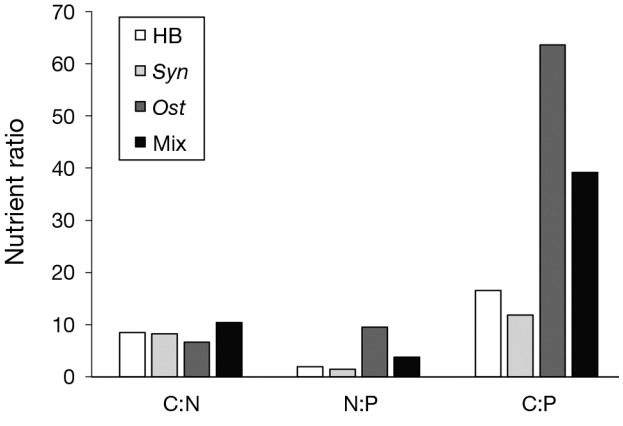

Fig. 3. Flagellate C:N, N:P and C:P ratios (n = 2) fed on varying prey. Abbreviations as in Figs. 1 & 2

3.3. Flagellate µ and IRs

Abundance estimates in the control bottles indicated low prey µ rates over the 24 h incubations (Table A1 in the Appendix). Average µ rates for the HNAN ranged from 0.9 to 1.8 d^{-1} across HB abundances from 10^3 to 10^6 cells ml^{-1} (Table 5). However, the only significant increase ($p < 0.05$) was detected comparing µ rates at 10^3 cells ml^{-1} to all other treatments. Feeding on *Syn* and *Ost* over increasing prey densities yielded average µ rates from 0.8 to 1.2 d^{-1} and from 1.1 to 1.4 d^{-1}, respectively, showing a continued increase of HNAN µ with prey density except for *Ost*, where µ seemed to level off at the 2 highest prey abundance treatments (Fig. 4, Table 5). Pro-

Table 5. Specific growth rate and ingestion rate (IR) for the flagellate (flag) averaged over triplicate incubations ±SD (see exact grazer and prey abundances in Table 1). HB: heterotrophic bacteria; *Syn*: *Synechococcus*; *Ost*: *Ostreococcus lucimarinus*; Mix: mixed prey assemblage

Prey	Prey (cells ml^{-1})	Flagellate μ (d^{-1})	IR (cells flag^{-1} d^{-1})	IR (pg C flag^{-1} d^{-1})	IR (pg N flag^{-1} d^{-1})	IR (pg P flag^{-1} d^{-1})
HB	10^3	0.9 ± 0.2	4 ± 0.2	0.28 ± 0.02	0.04 ± 0.00	0.02 ± 0.00
	10^4	1.6 ± 0.3	16 ± 3	1.19 ± 0.21	0.19 ± 0.03	0.08 ± 0.01
	10^5	1.7 ± 0.1	235 ± 62	18.06 ± 4.80	2.89 ± 0.75	1.17 ± 0.31
	10^6	1.8 ± 0.4	647 ± 109	49.87 ± 8.41	7.77 ± 1.31	3.24 ± 0.55
Syn	10^3	0.8 ± 0.1	1.0 ± 1	0.23 ± 0.12	0.05 ± 0.02	0.01 ± 0.00
	10^4	1.1 ± 0.8	51 ± 61	11.67 ± 14.21	2.43 ± 2.97	0.36 ± 0.43
	10^5	1.2 ± 0.6	243 ± 80	56.01 ± 18.33	11.69 ± 3.83	1.7 ± 0.56
	10^6	0.9 ± 0.6	2109 ± 1015	485.15 ± 233.40	101.25 ± 49.70	14.76 ± 7.10
Ost	10^3	1.1 ± 0.1	1 ± 1	1.63 ± 1.47	0.09 ± 0.08	0.01 ± 0.01
	10^4	1.4 ± 0.1	21 ± 2	45.56 ± 4.79	2.59 ± 0.27	0.38 ± 0.04
	10^5	1.2 ± 0.7	116 ± 69	249.29 ± 148.57	14.19 ± 8.45	2.09 ± 1.25
	10^6	1.3 ± 0.3	106 ± 23	227.03 ± 48.75	12.92 ± 2.77	1.91 ± 0.41
Mix	HB 10^5	1.0 ± 0.2	HB 14 ± 3	HB 1.06 ± 0.25	HB 0.17 ± 0.04	HB 0.07 ± 0.02
	Syn 10^3	1.0 ± 0.2	*Syn* 0.4 ± 0.3	*Syn* 0.08 ± 0.06	*Syn* 0.02 ± 0.01	*Syn* 0.00 ± 0.00
	Ost 10^3	1.0 ± 0.2	*Ost* 1 ± 0.3	*Ost* 1.13 ± 0.62	*Ost* 0.06 ± 0.03	*Ost* 0.01 ± 0.01

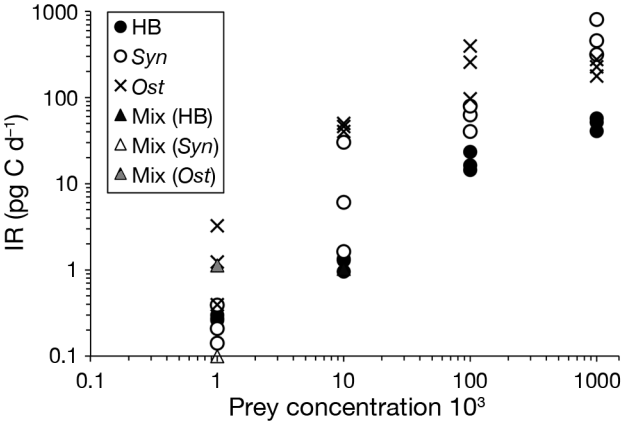

Fig. 4. Ingestion rate (IR; pg C flagellate^{-1} d^{-1}) at each of the initial prey concentrations (n = 36). Abbreviations as in Figs. 1 & 2

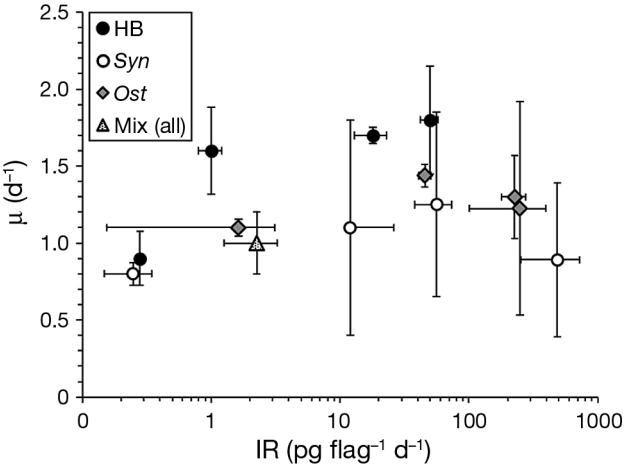

Fig. 5. C-based ingestion rates (IR; pg C flagellate^{-1} d^{-1}) in relation to flagellate growth (μ, d^{-1}). Also shown is the average for preying on the mixed assemblage ±SD. Note *x*-axis is log-transformed. Abbreviations as in Figs. 1 & 2

vided with mixed prey, HNAN μ averaged 1.0 d^{-1} (range = 0.8 to 1.3 d^{-1}) (Fig. 4, Table 5).

IRs, both computed using cell abundance and C estimates, generally increased with prey concentrations for all prey types with the exception of the *Ost* treatment at ~10^6 cells ml^{-1}, where IRs had started to decline (Table 5, Fig. 4). The HNAN reached its highest individual IRs with 647 ± 109 cells d^{-1} for HB, 2109 ± 1015 cells d^{-1} for *Syn* and 106 ± 23 d^{-1} cells for *Ost* (Table 5). Applying prey C conversion factors, maximal IRs corresponded to 50 ± 8 pg C flag^{-1} d^{-1} for HB, 485 ± 233 pg C flag^{-1} d^{-1} for *Syn* and 227 ± 49 pg C flag^{-1} d^{-1} for *Ost* (Table 5, Fig. 5). There was a significant difference in C-based IRs with *Ost* compared to both *Syn* and HB treatments at 10^4 and 10^5 cells ml^{-1} ($p < 0.05$). Additionally, there was a significant difference in C-based IRs between *Syn* and HB and *Syn* and *Ost* at 10^6 cells ml^{-1} ($p < 0.05$). Overall, IRs reached their highest for *Syn* at prey densities of ~10^5 cells ml^{-1}. In the mixed assemblage, *Ost* were grazed at the highest rates (1.13 ± 0.62 pg C flag^{-1} d^{-1}), followed by HB (1.06 ± 0.25 pg C flag^{-1} d^{-1}) and *Syn* (0.08 ± 0.06 pg C flag^{-1} d^{-1}). The IR calculated using N and P concentrations indicated that the *Syn* diet led to the highest intake of N (101.25 ± 49.70 pg N flag^{-1} d^{-1}), followed by *Ost* (14.19 ± 8.45 pg N flag^{-1} d^{-1}) and HB (7.77 ± 1.31 pg N flag^{-1} d^{-1}) (Table 5).

A *Syn* diet was also linked to the highest P uptake (14.76 ± 7.10 pg P flag^{-1} d^{-1}), followed by HB (3.24 ± 0.55 pg P flag^{-1} d^{-1}) and *Ost* (2.09 ±1.25 pg C flag^{-1} d^{-1}). In comparison, the mixed assemblage yielded lower average N- and P-based IRs, with HB reaching the highest rates of 0.17 ± 0.04 and 0.07 ± 0.02 flag^{-1} d^{-1}, respectively (Table 5).

Comparing across the single-prey treatments showed that flagellate μ increased with IRs up to ~50 pg C d^{-1} (range = 46–61 pg C d^{-1}, Fig. 5) but overall μ seemed constrained to <1.8 d^{-1} (Fig. 5). Despite the HNAN reaching average C-based IRs as high as 249 and 527 pg C flag^{-1} d^{-1} feeding on *Ost* and *Syn,* respectively, μ seemed to level off under the experimental conditions. The overall μ response of the flagellate in single-prey treatments remained the lowest at 0.8 d^{-1} which was its maximum for the *Syn* diet, compared to 1.4 and 1.8 d^{-1} for *Ost* and HB, respectively. The relatively high variability within each of the single-prey treatments rendered differences in μ nonsignificant ($p > 0.05$) (Fig. 4). HNAN μ on mixed prey fell into the mid-range of the overall observations at 1.0 d^{-1} and corresponded to a daily intake of 2.3 pg C flag^{-1} d^{-1} (Fig. 5).

3.4. GGE

Across all the treatments, average GGEs based on C estimates ranged from ~4 to 71%, and based on N and P, GGEs ranged from 2 to >100% and 11 to 89%, respectively (Fig. 6). C-based GGEs were highest when the flagellates were fed HB or a mixed prey assemblage compared to the *Syn* and *Ost* treatments ($p < 0.05$). N-based flagellate GGEs on a mixed diet exceeded those for all other diets ($p < 0.05$). Similarly, P-based GGEs were highest on mixed prey, followed by the HB treatment and, at considerably lower efficiencies, when the HNAN was offered *Syn* and *Ost* ($p < 0.05$).

4. DISCUSSION

4.1. Flagellate growth and ingestion

The newly-isolated HNAN demonstrated differential μ and IRs dependent on the prey that the flagellate was offered. Prey abundances for each of the prey types that fell below their 'typical' densities in coastal waters yielded low IRs, indicating that lower prey thresholds limit a prompt feeding response. While μ generally increased for the HNAN with

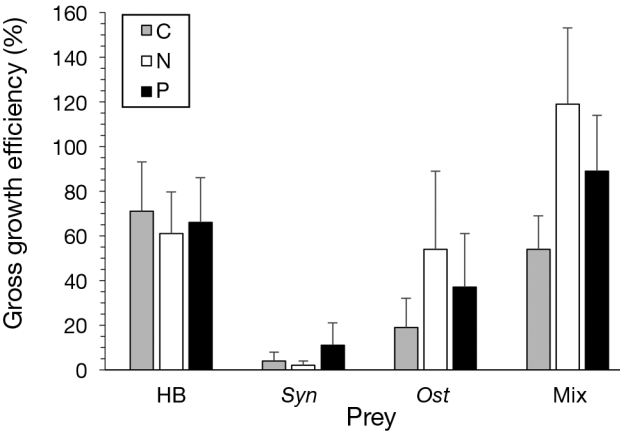

Fig. 6. Average flagellate gross growth efficiency (GGE) (C, N, P) grazing on HB, *Syn*, *Ost* and Mix (n = 3). Abbreviations as in Figs. 1 & 2

increased IRs of up to ~50 pg C d^{-1}, maximum μ seemed constrained to 1.8 d^{-1} when the flagellate fed on HB and peaked at ~1.4 d^{-1} feeding on *Ost* (Fig. 5). Despite the flagellate reaching its highest IRs with 485 pg C flag^{-1} d^{-1} feeding on *Syn*, its μ response was the lowest overall, leveling at ~1.3 d^{-1}. When all 3 prey organisms were offered together, the HNAN selected HB (1.1 ± 0.3 pg C flag^{-1} d^{-1}) and *Ost* (1.1 ± 0.6 pg C flag^{-1} d^{-1}) over *Syn* (0.1 ± 0.1 pg C flag^{-1} d^{-1}, Table 5). In a study by Guillou et al. (2001), single-prey experiments with *Syn* and with mixed prey for the HNAN *Picophagus flagellatus* showed similar outcomes; when *Syn* was offered alone, some of the lowest μ rates were recorded for *P. flagellatus* (0.6 d^{-1} compared to ~1.6 d^{-1} for the HNAN). In the same study, *Syn* was the preferred cyanobacterial choice when offered together with *Prochlorococcus* (Guillou et al. 2001). Here, regardless of whether IRs were based on C, N or P contents, the *Syn* treatment yielded the highest rates for the HNAN with the lowest μ. Since IRs based on different elements are rarely provided, we further compared IRs across studies using cell abundance changes (Table 6). IRs for *Syn* ranged from ~1 to 2109 cells flag^{-1} d^{-1} and exceeded previously reported rates of <1 to 57 cells flag^{-1} d^{-1} over similar prey densities (Table 6). For *Ost*, IRs ranged from 1 to 106 cells flag^{-1} d^{-1} and also exceeded most of the available published values ~6 to 19 cells flag^{-1} d^{-1} (Table 6). We took a closer look at the highest IR estimates for the HNAN in this study, which were observed when the flagellate fed on *Syn,* and calculated that these IRs would roughly equate to the ingestion of 1.5 *Syn* cells min^{-1}, or an average of ~40 s from contact to ingestion. Previously reported estimates on how long prey handling and ingestion can take compared well for HNANs of sim-

Table 6. Comparison table of growth (μ) and ingestion rates (IR) across various experiments with nanoflagellate species and picoplankton prey. The average or ranges are reported when available with standard deviation (±SD). Note: differences in experimental methodology exist between the studies. Empty cells with '–' indicate unavailable data. HNAN: heterotrophic nano-flagellate; HB: heterotrophic bacteria; *Syn*: *Synechococcus*; *Ost*: *Ostreococcus; Pro: Prochlorococcus*; Bact Cult: bacterial culture; *Chlor*: *Chlorocystis*

Nanoflagellate(s)	Prey	Flagellate abundance (cells ml^{-1})	Prey abundance (cells ml^{-1})	μ (d^{-1})	IR (cells $flagellate^{-1}$ d^{-1})	Temp (°C)	Duration (h)	Reference
Unknown HNAN	HB	4.6×10^2	3.4×10^3	0.9 ± 0.2	4 ± 0.2	16	24	This study
	HB	4.7×10^2	1.8×10^4	1.6 ± 0.3	16 ± 3	16	24	
	HB	2.8×10^2	1.7×10^5	1.7 ± 0.1	235 ± 62	16	24	
	HB	5.3×10^2	0.9×10^6	1.8 ± 0.4	647 ± 109	16	24	
	Syn	2.8×10^2	1.0×10^3	0.8 ± 0.1	1 ± 1	16	24	
	Syn	2.0×10^2	2.2×10^4	1.1 ± 0.8	51 ± 62	16	24	
	Syn	2.8×10^2	1.5×10^5	1.2 ± 0.6	243 ± 80	16	24	
	Syn	3.0×10^2	10×10^6	0.9 ± 0.6	2109 ± 1015	16	24	
	Ost	6.4×10^2	2.2×10^3	1.1 ± 0.1	1 ± 1	16	24	
	Ost	4.3×10^2	3.7×10^4	1.4 ± 0.1	21 ± 2	16	24	
	Ost	5.3×10^2	5.3×10^5	1.2 ± 0.7	116 ± 69	16	24	
	Ost	5.7×10^2	0.7×10^6	1.3 ± 0.3	106 ± 23	16	24	
Pseudobodo sp.	*Syn* WH8103	3.9×10^4	1.5×10^3–1.3×10^6	–	0.012–64	18	12	Christaki et al. (2002)
	Pro MED4	3.9×10^4	1.1×10^3–2.8×10^6	–	0.024–160	18	12	
Picophagus flagellates[a]	*Pro* SS120	2.3×10^4	5.2×10^5	1.6	28	19	10	Guillou et al. (2001)
	Syn WH8103	2.4×10^3	2.7×10^5	0.6	16	19	10	
	Pro SS120	2.8×10^4	2.6×10^5	1.5	9	19	10	
	Syn WH8103	2.8×10^4	1.2×10^4	1.5	9	19	10	
Jakoba libera	*Ost*	4.5×10^2	0.5×10^6	1.2	15	18	60–114	Christaki et al. (2005)
Cafeteria and *Monosiga* sp.	*Ost*	2.3×10^2	1.9×10^6	3.1	19	18	60–114	
P. imperforata	Bact Cult	9.4×10^4–2.5×10^5	3–6.7×10^8	2.7 ± 0.08	1488 ± 117	15	18–36	Choi & Peters (1992)
	Bact Cult	9.4×10^4–2.5×10^5	3–6.7×10^8	2.3 ± 0.12	2376 ± 237	15	18–36	
	Bact Cult	9.4×10^4–2.5×10^5	3–6.7×10^8	0.9 ± 0.07	480 ± 36	6	18–36	
	Bact Cult	9.4×10^4–2.5×10^5	3–6.7×10^8	1.5 ± 0.11	1320 ± 194	6	18–36	
	Bact Cult	9.4×10^4–2.5×10^5	3–6.7×10^8	0.5 ± 0.07	336 ± 98	–1.5	18–36	
	Bact Cult	9.4×10^4–2.5×10^5	3–6.7×10^8	0.8 ± 0.03	720 ± 72	–1.5	18–36	
P. imperforata	Bact Cult	2×10^3	8×10^5–2.2×10^8	5.0	–	20	48	Eccleston-Parry & Leadbeater (1994)
Spumella sp.	Bact Cult	1–2×10^3	2×10^8	0.3 ± 0.17	–	16	15	Boenigk et al. (2006)
	Bact Cult	1–2×10^3	2×10^8	2.8 ± 0.06	–	16	15	
Mixed	*Syn* WH8103	3.4×10^4	1.2×10^3–1.4×10^4	–	0.005–57	18	12	Christaki et al. (2002)
	Pro MED4	3.4×10^4	1.9×10^3–2.7×10^6	–	0.05–153	18	12	
Mixed	*Ost*	4.2×10^4	0.3×10^6	–	6	18	0–144	Christaki et al. (2005)
	Syn WH8103	4.2×10^4	2.7×10^6	–	19.2	18	24–96	

[a]Flagellates that are known mixotrophs

ilar size (3–8 µm). *Cafeteria roenbergensis*, *Bodo sultans* and *Ochromonas* sp. averaged ~2 to 14 s from contact to ingestion of prey, equivalent to 4–39 prey cells min^{-1} (Boenigk & Arndt 2000).

4.2. Flagellate cell stoichiometry, BV and GGE

The HNAN varied in its nutrient composition dependent on the prey that was offered. Overall C:N:P ratios from 12:1:1 to 64:10:1 fell well within the wide range seen in studies that incorporated direct measurements of cell stoichiometry (Table 3). It is worth noting that our individual CNP measurements for both prey and grazer compared well to previously published data for HB, *Syn* and HNANs (Kana & Glibert 1987, Lee & Fuhrman 1987, Eccleston-Parry & Leadbeater 1995, Theil-Nielsen & Søndergaard 1998, Bertilsson et al. 2003). For *Ost*, cellular C and N concentrations were higher than published rates of ~233–247 fg C $µm^{-3}$ and ~50 fg N $µm^{-3}$ (Worden et al. 2004, Liefer et al. 2019) but still fell within the wide range reported for picoeukaryotes (Zubkov et al. 1998). In this study, the relatively low P content in *Ost* (C:P ratios of 119:1 for *Ost* compared to 14:1 and 31:1 for HB and *Syn*, respectively; Fig. 3, Table 4) drove a shift in C:N:P ratios of the HNAN in both the single-prey experiment and when offered a mixed prey assemblage (Table 3). Similarly, a study by Chrzanowski et al. (2010) reported a shift in cellular composition for an HNAN species grazing on HB of varying nutrient content. Fed on *Pseudomonas fluorescens* raised under balanced nutrient conditions, the HNAN *Ochromonas danica* yielded C:N:P ratios of 161:10:1 compared to 80:12:1 when the bacterium grew under C-limited conditions before being offered to the flagellate (Chrzanowski et al. 2010).

Previous studies also linked shifts in HNAN stoichiometry and differences in incorporation efficiencies to the specific grazer species (Grover 2004, Chrzanowski & Foster 2014). For instance, Eccleston-Parry & Leadbeater (1995) showed cellular C:N:P ratios of 71:13:1 for *Jakoba libera* in contrast to 6:2:1 for *Bodo designis* feeding on the same HB assemblage (Eccleston-Parry & Leadbeater 1995). Dissolved organic matter egestion studies, both with phototrophic and heterotrophic prey, have also shown that a higher release of P compared to either C or N may be observed dependent on prey type (Andersson et al. 1985, Nagata & Kirchman 1991, Ferrier-Pages et al. 1998). For instance, while grazing on phytoplankton, the HNAN *Paraphysomonas imperforata* released 10% of the ingested C (Caron et al. 1985) and 15–20% of the ingested P as dissolved fractions (Anderson & Gardner 1986). Conversely, when grazing on bacteria, *P. imperforata* released 8–27% of C (Chase & Price 1997), 22% of N (Nagata & Kirchman 1991) and 70% of total P (Anderson & Gardner 1986). Achieving better resolution of these complex prey–predator specific stoichiometric relationships will require a move away from previously published, fixed conversion factors, since cell nutrient concentrations can vary significantly (Choi & Peters 1992, Pelegrí et al. 1999, Selph et al. 2003).

Our study demonstrated that HNAN µ on varying prey was also linked to changes in flagellate BV. In the single-prey treatments, the HNAN had the highest increase in cell BV (79%) by the end of the experiment while grazing on *Syn*. Overall, a *Syn* diet not only resulted in the highest IRs but also major BV increases, while yielding the lowest HNAN µ rates. All together, these findings signified the limited ability of HNANs to fully digest and assimilate *Syn*, which was also reflected in low GGEs (2–11% for C, N and P) compared to the HB (61–71%) and *Ost* GGEs (19–54%) (Fig. 6). Low incorporation efficiency due to inefficient prey processing and subsequent egestion (Dolan & Šimek 1998, Shannon et al. 2007) has been previously linked to low GGEs dependent on the prey type (Pelegrí et al. 1999). This study corroborates that certain *Syn* strains may adversely impact HNAN population µ and fitness (Gorsky et al. 1999, Guillou et al. 2001, Shannon et al. 2007, Apple et al. 2011).

Overall, and not surprisingly, the HNAN seemed to benefit from being offered mixed prey (GGEs ranging from 54 to >100%; Fig. 6), since having a more diverse prey assemblage available increased the likelihood that all dietary requirements (C, N, P, Fe, etc.) were met (DeMott 1998, Gamfeldt et al. 2005, Striebel et al. 2012, Yang et al. 2019). The significant increase in HNAN BV in the mixed treatment paired with modest µ seemed to be related to the presence of *Syn* being ingested as part of the prey assemblage. Since the size of HNANs can affect their own susceptibility to grazers, where larger cells are selected for (Samuelsson & Andersson 2003), these diet-induced shifts in HNAN size may also impact C flow to higher trophic levels.

4.3. Impact on picoplankton standing stocks

Daily C removal rates were calculated employing average HNAN IRs from the single prey treatment and assuming natural abundances of HB (10^5 cells ml^{-1}), *Syn* (10^3 cells ml^{-1}), *Ost* (10^3 cells ml^{-1}) and the

HNAN (10^3 cells ml^{-1}). This would have resulted in a daily removal estimate of >100% of HB standing stocks consumed and 2 and 16% of *Syn* and *Ost* biomass grazed, respectively. These estimates changed when we used the IRs from the mixed prey trial experiment, which could be considered a slightly better representation of natural feeding conditions. Here, HNAN IRs extrapolated to a daily removal of 11% of the HB standing stock, 1 and 11% of *Syn* and *Ost* C biomass being grazed, respectively. Previous studies reported average removal rates of incident HB populations with 45–87% and maxima of >100% in coastal waters (Šolić & Krstulović 1994, Christaki et al. 2001). Similar to our estimate, previous laboratory and field studies in coastal subtropical and oligotrophic waters suggested lower removal with 1–20% of C standing stocks and a maximum of 45% for *Syn* (Safi & Hall 1999, Christaki et al. 2001). There are currently no comparative studies that estimate grazing impact of heterotrophic flagellates on *in situ Ost* populations, but this study suggested that HNAN grazing could account for losses (~16%).

In summary, we present data on μ, IR and GGEs for a newly isolated, not yet fully characterized, HNAN under various diet regimes, highlighting the importance of prey-specific approaches when resolving trophic interactions within the microbial loop. Flagellate diet choices affected grazer stoichiometry, and the choice of prey type had consequences for the BV of the flagellate. In turn, these BV changes likely impact flagellate grazer dynamics and carbon flow to higher trophic levels. Our study highlights the importance of direct stoichiometric observations to link how prey–predator interactions may alter energy flux. Ongoing work will allow for the full taxonomic characterization of the flagellate, and future studies will focus on determining its contribution to natural flagellate communities and in relation to environmental conditions in coastal waters of North Carolina.

Acknowledgements. This work was partially supported by National Science Foundation grant OCE-1459406. We thank Claudia Benitez-Nelson for support on C:N:P analyses. A graduate fellowship by the Department of the Interior Southeast Climate Adaptation Science Center and a Doctoral Dissertation Completion Grant by North Carolina State University were awarded to G.L.C. We thank the editor and reviewers for their thoughtful comments and their efforts towards improving our manuscript.

LITERATURE CITED

Anderson JT, Gardner GA (1986) Plankton communities and physical oceanography observed on the Southeast Shoal region, Grand Bank of Newfoundland. J Plan Res 8: 1111–1135

Andersson A, Lee C, Azam F, Hagström Å (1985) Release of amino acids and inorganic nutrients by heterotrophic marine microflagellates. Mar Ecol Prog Ser 23:99–106

Apple JK, Strom SL, Palenik B, Brahamsha B (2011) Variability in protist grazing and growth on different marine *Synechococcus* isolates. Appl Environ Microbiol 77: 3074–3084

Aspila KI, Agemian H, Chau ASY (1976) A semi-automated method for the determination of inorganic, organic and total phosphate in sediments. Analyst 101:187–197

Azam F, Fenchel T, Field JG, Gray JS, Meyer-Reil LA, Thingstad F (1983) The ecological role of water-column microbes in the sea. Mar Ecol Prog Ser 10:257–263

Bec A, Martin-Creuzburg D, von Elert E (2006) Trophic upgrading of autotrophic picoplankton by the heterotrophic nanoflagellate *Paraphysomonas* sp. Limnol Oceanogr 51:1699–1707

Benitez-Nelson CR, Madden LPN, Styles RM, Thunell RC, Astor Y (2007) Inorganic and organic sinking particulate phosphorus fluxes across the oxic/anoxic water column of Cariaco Basin, Venezuela. Mar Chem 105:90–100

Bertilsson S, Berglund O, Karl DM, Chisholm SW (2003) Elemental composition of marine *Prochlorococcus* and *Synechococcus*: implications for the ecological stoichiometry of the sea. Limnol Oceangr 48:1721–1731

Boenigk J, Arndt H (2000) Particle handling during interception feeding by four species of heterotrophic nanoflagellates. J Eukaryot Microbiol 47:350–358

Boenigk J, Matz C, Jürgens K, Arndt H (2001) The influence of preculture conditions and food quality on the ingestion and digestion process of three species of heterotrophic nanoflagellates. Microb Ecol 42:168–176

Boenigk J, Pfandl K, Hansen PJ (2006) Exploring strategies for nanoflagellates living in a 'wet desert'. Aquat Microb Ecol 44:71–83

Børsheim KY, Bratbak G (1987) Cell volume to cell carbon conversion factors for a bacterivorous *Monas* sp. enriched from seawater. Mar Ecol Prog Ser 36:171–175

Bratvold D, Srienc F, Taub SR (2000) Analysis of the distribution of ingested bacteria in nanoflagellates and estimation of grazing rates with flow cytometry. Aquat Microb Ecol 21:1–12

Bręk-Laitinen G, Ojala A (2011) Grazing of heterotrophic nanoflagellates on the eukaryotic picoautotroph *Choricystis* sp. Aquat Microb Ecol 62:49–59

Caron DA, Goldman JC, Andersen OK, Dennett MR (1985) Nutrient cycling in a microflagellate food chain: II. Population dynamics and carbon cycling. Mar Ecol Prog Ser 24:243–254

Caron DA, Porter KG, Sanders RW (1990) Carbon, nitrogen, and phosphorus budgets for the mixotrophic phytoflagellate *Poterioochromonas malhamensis* (Chrysophyceae) during bacterial ingestion. Limnol Oceanogr 35: 433–443

Caron DA, Peele ER, Lim EL, Dennett MR (1999) Picoplankton and nanoplankton and their trophic coupling in surface waters of the Sargasso Sea south of Bermuda. Limnol Oceanogr 44:259–272

Chase Z, Price NM (1997) Metabolic consequences of iron deficiency in heterotrophic marine protozoa. Limnol Oceanogr 42:1673–1684

Choi JW, Peters F (1992) Effects of temperature on two psychrophilic ecotypes of a heterotrophic nanoflagellate,

Paraphysomonas imperforata. Appl Environ Microbiol 58:593–599

Christaki U, Giannakourou A, Van Wambeke F, Grégori G (2001) Nanoflagellate predation on auto-and heterotrophic picoplankton in the oligotrophic Mediterranean Sea. J Plankton Res 23:1297–1310

Christaki U, Courties C, Karayanni H, Giannakourou A, Maravelias C, Kormas KA, Lebaron P (2002) Dynamic characteristics of *Prochlorococcus* and *Synechococcus* consumption by bacterivorous nanoflagellates. Microb Ecol 43:341–352

Christaki U, Vázquez-Domínguez E, Courties C, Lebaron P (2005) Grazing impact of different heterotrophic nanoflagellates on eukaryotic (*Ostreococcus tauri*) and prokaryotic picoautotrophs (*Prochlorococcus* and *Synechococcus*). Environ Microbiol 7:1200–1210

Chrzanowski TH, Foster BLL (2014) Prey element stoichiometry controls ecological fitness of the flagellate *Ochromonas danica.* Aquat Microb Ecol 71:257–269

Chrzanowski TH, Lukomski NC, Grover JP (2010) Element stoichiometry of a mixotrophic protist grown under varying resource conditions. J Eukaryot Microbiol 57: 322–327

Countway PD, Caron DA (2006) Abundance and distribution of *Ostreococcus* sp. in the San Pedro Channel, California, as revealed by quantitative PCR. Appl Environ Microbiol 72:2496–2506

Dahlgren K, Andersson A, Larsson U, Hajdu S, Båmstedt U (2010) Planktonic production and carbon transfer efficiency along a north–south gradient in the Baltic Sea. Mar Ecol Prog Ser 409:77–94

DeMott WR (1998) Utilization of a cyanobacterium and a phosphorus-deficient green alga as complementary resources by daphnids. Ecology 79:2463–2481

Dolan JR, Šimek K (1998) Ingestion and digestion of an autotrophic picoplankter, *Synechococcus*, by a heterotrophic nanoflagellate, *Bodo saltans*. Limnol Oceanogr 43: 1740–1746

Dolan JR, Šimek K (1999) Diel periodicity in *Synechococcus* populations and grazing by heterotrophic nanoflagellates: analysis of food vacuole contents. Limnol Oceanogr 44:1565–1570

Eccleston-Parry JD, Leadbeater BS (1994) A comparison of the growth kinetics of six marine heterotrophic nanoflagellates fed with one bacterial species. Mar Ecol Prog Ser 105:167–177

Eccleston-Parry JD, Leadbeater B (1995) Regeneration of phosphorus and nitrogen by four species of heterotrophic nanoflagellates feeding on three nutritional states of a single bacterial strain. Appl Environ Microbiol 61:1033–1038

Fenchel T (1982a) Ecology of heterotrophic microflagellates. II. Bioenergetics and growth. Mar Ecol Prog Ser 8: 225–231

Fenchel T (1982b) Ecology of heterotrophic microflagellates. IV. Quantitative occurrence and importance as bacterial consumers. Mar Ecol Prog Ser 9:35–42

Ferrier-Pagès C, Karner M, Rassoulzadegan F (1998) Release of dissolved amino acids by flagellates and ciliates grazing on bacteria. Oceanol Acta 21:485–494

Froelich PN (1980) Analysis of organic carbon in marine sediments. Limnol Oceanogr 25:564–572

Frost B (1972) Effects of size and concentration of food particles on the feeding behavior of the marine planktonic copepod *Calanus pacificus*. Limnol Oceanogr 17:805–815

Gamfeldt L, Hillebrand H, Jonsson PR (2005) Species richness changes across two trophic levels simultaneously affect prey and consumer biomass. Ecol Lett 8:696–703

Gonzalez JM, Sherr EB, Sherr BF (1990) Size-selective grazing on bacteria by natural assemblages of estuarine flagellates and ciliates. Appl Environ Microbiol 56:583–589

Gorsky G, Chrétiennot-Dinet M, Blanchot J, Palazzoli I (1999) Picoplankton and nanoplankton aggregation by appendicularians: fecal pellet contents of *Megalocercus huxleyi* in the equatorial Pacific. J Geophys Res Oceans 104:3381–3390

Grover JP (2004) Predation, competition, and nutrient recycling: a stoichiometric approach with multiple nutrients. J Theor Biol 229:31–43

Grover JP, Chrzanowski TH (2009) Dynamics and nutritional ecology of a nanoflagellate preying upon bacteria. Microb Ecol 58:231–243

Guillard RRL, Ryther JH (1962) Studies of marine planktonic diatoms: I. *Cyclotella nana* Hustedt, and *Detonula confervacea* (Cleve) Gran. Can J Microbiol 8:229–239

Guillou L, Jacquet S, Chrétiennot-Dinet MJ, Vaulot D (2001) Grazing impact of two small heterotrophic flagellates on *Prochlorococcus* and *Synechococcus*. Aquat Microb Ecol 26:201–207

Heinbokel J (1978) Studies on the functional role of tintinnids in the Southern California Bight. I. Grazing and growth rates in laboratory cultures. Mar Biol 47:177–189

Hillebrand H, Dürselen CD, Kirschtel D, Pollingher U, Zohary T (1999) Biovolume calculation for pelagic and benthic microalgae. J Phycol 35:403–424

Hondeveld BJM, Bak RPM, Van Duyl FC (1992) Bacterivory by heterotrophic nanoflagellates in marine sediments measured by uptake of fluorescently labeled bacteria. Mar Ecol Prog Ser 89:63–71

Kana TM, Glibert PM (1987) Effect of irradiances up to 2000 µE m^{-2} s^{-1} on marine *Synechococcus* WH7803—I. Growth, pigmentation, and cell composition. Deep-Sea Res A Oceanogr Res Pap 34:479–495

Karayanni H, Christaki U, Van Wambeke F, Denis M, Moutin T (2005) Influence of ciliated protozoa and heterotrophic nanoflagellates on the fate of primary production in the northeast Atlantic Ocean. J Geophys Res 110:C07S15

Lee S, Fuhrman JA (1987) Relationships between biovolume and biomass of naturally derived marine bacterioplankton. Appl Environ Microbiol 53:1298–1303

Liefer JD, Garg A, Fyfe MH, Irwin AJ and others (2019) The macromolecular basis of phytoplankton C:N:P under nitrogen starvation. Front Microbiol 10:763

Nagata T, Kirchman DL (1991) Release of dissolved free and combined amino acids by bacterivorous marine flagellates. Limnol Oceanogr 36:433–443

Olson RJ, Chisholm SW, Zettler ER, Armbrust EV (1990) Pigments, size, and distributions of *Synechococcus* in the North Atlantic and Pacific Oceans. Limnol Oceanogr 35: 45–58

Pelegrí SP, Christaki U, Dolan J, Rassoulzadegan F (1999) Particulate and dissolved organic carbon production by the heterotrophic nanoflagellate *Pteridomonas danica* Patterson and Fenchel. Microb Ecol 37:276–284

Pernthaler J (2005) Predation on prokaryotes in the water column and its ecological implications. Nat Rev Microbiol 3:537

Pomeroy LR (1974) The ocean's food web, a changing paradigm. Bioscience 24:499–504

Porter KG, Feig YS (1980) The use of DAPI for identifying and counting aquatic microflora. Limnol Oceanogr 25:943–948
Rose JM, Vora NM, Countway PD, Gast RJ, Caron DA (2009) Effects of temperature on growth rate and gross growth efficiency of an Antarctic bacterivorous protist. ISME J 3:252
Safi KA, Hall JA (1999) Mixotrophic and heterotrophic nanoflagellate grazing in the convergence zone east of New Zealand. Aquat Microb Ecol 20:83–93
Samuelsson K, Andersson A (2003) Predation limitation in the pelagic microbial food web in an oligotrophic aquatic system. Aquat Microb Ecol 30:239–250
Schnepf E, Kühn S (2000) Food uptake and fine structure of *Cryothecomonas longipes* sp. nov., a marine nanoflagellate incertae sedis feeding phagotrophically on large diatoms. Helgol Mar Res 54:18–32
Selph KE, Landry MR, Laws EA (2003) Heterotrophic nanoflagellate enhancement of bacterial growth through nutrient remineralization in chemostat culture. Aquat Microb Ecol 32:23–37
Shannon SP, Chrzanowski TH, Grover JP (2007) Prey food quality affects flagellate ingestion rates. Microb Ecol 53: 66–73
Šimek K, Chrzanowski TH (1992) Direct and indirect evidence of size-selective grazing on pelagic bacteria by freshwater nanoflagellates. Appl Environ Microbiol 58: 3715–3720
Sin Y, Webb KL, Sieracki ME (1998) Carbon and nitrogen densities of the cultured marine heterotrophic flagellate *Paraphysomonas* sp. J Microbiol Methods 34:151–163
Šolić M, Krstulović N (1994) Role of predation in controlling bacterial and heterotrophic nanoflagellate standing stocks in the coastal Adriatic Sea: seasonal patterns. Mar Ecol Prog Ser 114:219–235
Straile D (1997) Gross growth efficiencies of protozoan and metazoan zooplankton and their dependence on food concentration, predator–prey weight ratio, and taxonomic group. Limnol Oceanogr 42:1375–1385
Striebel M, Singer G, Stibor H, Andersen T (2012) 'Trophic overyielding': phytoplankton diversity promotes zooplankton productivity. Ecology 93:2719–2727
Theil-Nielsen J, Søndergaard M (1998) Bacterial carbon biomass calculated from biovolumes. Arch Hydrobiol 141: 195–207
Tsai A, Gong GC, Hung J (2013) Seasonal variations of virus- and nanoflagellate-mediated mortality of heterotrophic bacteria in the coastal ecosystem of subtropical western Pacific. Biogeosciences 10:3055–3065
Weekers PH, Gast RJ, Fuerst PA, Byers TJ (1994) Sequence variations in small-subunit ribosomal RNAs of *Hartmannella vermiformis* and their phylogenetic implications. Mol Biol Evol 11:684–690
White TJ, Bruns T, Lee S, Taylor J (1990) Amplification and direct sequencing of fungal ribosomal RNA genes for phylogenetics. In: Innis MA, Gelfand DH, Sninsky JJ, White TJ (eds) PCR protocols: a guide to methods and applications. Academic Press, New York, NY, p 315–322
Wikner J, Andersson A, Normark S, Hagström Å (1986) Use of genetically marked minicells as a probe in measurement of predation on bacteria in aquatic environments. Appl Environ Microbiol 52:4–8
Worden AZ (2006) Picoeukaryote diversity in coastal waters of the Pacific Ocean. Aquat Microb Ecol 43:165–175
Worden AZ, Nolan JK, Palenik B (2004) Assessing the dynamics and ecology of marine picophytoplankton: the importance of the eukaryotic component. Limnol Oceanogr 49:168–179
Yang J, Löder MGJ, Jiang Y, Wiltshire KH (2019) Are tintinnids picky grazers: feeding experiments on a mixture of mixotrophic dinoflagellates and implications for red tide dynamics. Mar Pollut Bull 149:110488
Zar JH (1984) Biostatistical analysis. Prentice-Hall, Englewood Cliffs, NJ
Zubkov MV, Sleigh MA, Tarran GA, Burkill PH, Leakey RJ (1998) Picoplanktonic community structure on an Atlantic transect from 50° N to 50° S. Deep Sea Res I 45: 1339–1355
Zwirglmaier K, Spence E, Zubkov MV, Scanlan DJ, Mann NH (2009) Differential grazing of two heterotrophic nanoflagellates on marine *Synechococcus* strains. Environ Microbiol 11:1767–1776

Appendix. Additional data

Table A1. Prey growth (μ d^{-1}) in control treatments shown as average ± SD. HB: heterotrophic bacteria; *Syn*: *Synechococcus*; *Ost*: *Ostreococcus lucimarinus*; Mix: mixed prey assemblage with the individual prey growth rates within the assemblage

Prey	μ
HB	0.03 ± 0.08
Syn	−0.02 ± 0.1
Ost	0.1 ± 0.1
Mix (HB)	0.01 ± 0.01
Mix (*Syn*)	0.003 ± 0.003
Mix (*Ost*)	−0.03 ± 0.01

Editorial responsibility: Toshi Nagata, Kashiwanoha, Japan
Reviewed by: 3 anonymous referees

Submitted: March 22, 2021
Accepted: October 6, 2021
Proofs received from author(s): December 27, 2021